

# Interband optical transitions in GaAs-Ga<sub>1-x</sub>Al<sub>x</sub>As superlattices in an applied electric field

B. Jogai and K. L. Wang

*Device Research Laboratory, Department of Electrical Engineering, University of California at Los Angeles,  
Los Angeles, California 90024*

(Received 11 July 1986)

We have investigated the light absorption in a GaAs-Ga<sub>1-x</sub>Al<sub>x</sub>As superlattice in the presence of an applied electric field. Using Houston functions to represent the valence and conduction states we have calculated the transition rates between the valence and conduction subbands for different values of the field. Both the Franz-Keldysh shift and Franz-Keldysh oscillations emerge from the formalism. The absorption edge as a function of photon energy varies exponentially and has small oscillations superimposed on it. It is followed by a flat region characteristic of a two-dimensional electron gas. The use of Houston functions is justified by computing the tunneling probability between adjacent subbands and showing that it is negligibly small.

## I. INTRODUCTION

Light absorption in superlattices and quantum wells in the presence of an electric field has been investigated in the recent literature for possible applications in electro-optics. Recent experiments have shown that the absorption coefficient is strongly affected by an applied electric field.<sup>1-4</sup> The modulation of the absorption coefficient has led to the proposal of a new class of switching devices<sup>3,5</sup> which can be operated by changing the field applied to the superlattice structure, thereby creating "on" and "off" transmission states for the light wave. In the superlattice case absorption can occur for photon energies both above and below the superlattice band gap. The latter is the usual Franz-Keldysh effect.<sup>6,7</sup> Unlike bulk material, the absorption edge is anticipated to be more sensitive to the field, a consequence of the lowering of the effective superlattice band gap. This effect originates from the polarization of the superlattice envelope function by the electric field and may be of the order of a few meV. For bulk material, on the other hand, the effect is small because the host Bloch functions are not seriously distorted for fields below the avalanche breakdown. Switching can thus be effected using a superlattice for photon energies below the band gap since the electric field can be used to turn the transmission on and off. The feasibility of switching below the band gap depends on the sensitivity of the absorption coefficient to the field. Assuming that the large device capacitance can be circumvented to allow fast switching, these devices may be useful for integrated optics, hence the need for further studies of the electroabsorption effect in superlattices.

The purpose of this paper is to investigate the electroabsorption in GaAs-Ga<sub>1-x</sub>Al<sub>x</sub>As superlattices. Using the theory of light-assisted tunneling, we have calculated the absorption coefficient for photon energies below and above the superlattice band gap. Among the recent work in this area, two sets of calculations in particular have addressed the problem of modeling the electric field in the superlattice and multiple quantum well (MQW) in some detail.<sup>8,9</sup> In these articles, the absorption coefficient and

wave-function overlaps have been worked out using suitable model potentials to represent the superlattice and MQW. In Ref. 8 the Ga<sub>1-x</sub>Al<sub>x</sub>As layers are considered sufficiently thick that the electrons and holes cannot tunnel between adjacent wells. In fact Miller *et al.*<sup>8</sup> considered the ideal case where the potential barrier is infinite. The electric field was incorporated by tilting the bottom of the well. The authors then computed the red shift and showed from their bound-state model the closeness between the Stark shift and the Franz-Keldysh effect. McIlroy<sup>9</sup> calculated the change in overlap between the electrons and holes in an MQW caused by an electric field, a prerequisite to understanding the electroabsorption phenomenon in these structures. McIlroy imposed an artificial boundary condition on the MQW by sandwiching it between semi-infinite barrier layers having constant potentials. Since both approaches are essentially bound-state models, they yield absorption coefficients that consist of a superposition of step functions and are characterized by abrupt increases as the photon energy is increased. Such results are characteristic of the two-dimensional bound-state problem and are a consequence of the electron being unable to tunnel out of the structure. When an electric field is applied, the function is simply shifted to the left. In the conventional terminology, this is due to the Stark lowering of the bound electron and hole states. But as pointed out in Refs. 8 and 9, once a field is applied, there are no true bound states. This is especially true for the superlattice and MQW where the barrier heights are small (typically around 0.25 eV). And since the particles now exist in the quasibound states for only a short time (e.g., 10<sup>-13</sup> s), the problem is essentially similar to the bulk (i.e., three dimensional) and therefore a considerable smearing out of the steplike behavior is expected. Conventionally, the red shift with increasing field for continuum states is the Franz-Keldysh effect. For the superlattice and MQW the two effects are clearly related. However in this paper we denote the red shift in our model as the Franz-Keldysh effect in keeping with the usual notation.

Our calculations differ from those of Refs. 8 and 9 in the important aspect of boundary conditions; we avoid the use of restrictive end conditions (usually necessary for

wave-function normalization) on the superlattice. In principle one could cope with the problem of normalization by placing the superlattice or MQW in the middle of a large box (say, 1000 nm wide) having infinite walls. But this raises the problem that the superlattice or MQW will only constitute a small fraction of the total structure and may therefore have very little bearing on the final result. In our approach this problem does not occur since our model is not that of a particle in a box. We assume that the superlattice consists of a sufficiently large number of layers that periodicity can be assumed, and that the electrons and holes experience a constant field throughout, in a direction parallel to the growth axis. Furthermore, we treat the case of relatively thin barriers where coupling between the quantum wells needs to be accounted for. We point out that coupling between wells is implicit in Ref. 9 in which the total wave function of the system is constructed.

As a simplification we neglect the excitonic transitions. For the MQW the absorption spectra is dominated by excitonic peaks as shown in the literature, but as the barriers become thinner, there is a tendency for the peaks to be smeared out, as demonstrated by Dingle *et al.*<sup>10</sup> However, the Coulomb interaction between electrons and holes remains and produces a correction to the absorption coefficient. We have not included this effect. Our treatment of the electric field differs from that of previous authors in that it is similar to the bulk treatise. In previous MQW and superlattice models the field was introduced by tilting the wells and then making certain assumptions about the field in the end regions. In most instances the outer regions are assumed to be thick layers of  $\text{Ga}_{1-x}\text{Al}_x\text{As}$  in which the field is allowed to vanish beyond a certain distance. It affords some convenience in modeling as one need not worry about the wave function leaking out of the end regions. But the overall effect is somewhat similar to creating an internal electric field by varying the Al concentration, and would seem to be a local-field effect instead of a global effect produced by an externally applied field. Furthermore, the results will depend on the choice of assumptions for the boundaries. In this paper we offer an alternative approach. Our results show the Franz-Keldysh shift when the photon energy is less than the superlattice band gap, and Franz-Keldysh oscillations when the energy is above the band gap. The absorption below the band gap shown here is the same as photoassisted tunneling in bulk material.

In Sec. II we calculate the interband transition rate between the Houston states representing the conduction and valence bands. Band mixing caused by the electric field would tend to invalidate our approach. Accordingly, in Sec. III we have investigated the interband coupling by calculating the tunneling probability between adjacent subbands for moderate values of electric field. Results are shown in Sec. IV.

## II. METHOD

We use Houston functions<sup>11</sup> to represent the superlattice states. An alternative scheme for bulk material uses stationary wave functions.<sup>12</sup> In the absence of interband coupling the two approaches yield identical results.<sup>6,7,12</sup>

The use of Houston functions allows us to conveniently include the nonparabolicity of the subbands. Using a simple effective mass scheme we construct the superlattice conduction-band states from

$$\Psi_{cn}(\mathbf{k}_\perp, q, r, \tau) = \frac{1}{\sqrt{S}} u_c \exp(i\mathbf{k}_\perp \cdot \mathbf{r}_\perp) f_{cn} \times \exp \left[ -\frac{i}{\hbar} \int_0^\tau E_{cn}(\mathbf{k}_\perp, q) d\tau' \right], \quad (1)$$

where  $u_c$  is the cell periodic part of the host Bloch function at the zone center,  $\mathbf{k}_\perp$  is the wave vector in the  $y$ - $z$  plane,  $q$  is the wave vector in the  $x$  direction,  $\tau$  is the elapsed time, and  $S$  is the cross-sectional area in the superlattice plane.  $f_{cn}$  is an envelope function which accounts for the band-edge perturbation, and  $n$  labels the superlattice subbands. Under the action of the electric field  $F$ , the wave-vector changes in the manner  $\hbar\mathbf{q}(\tau) = \hbar\mathbf{q}(\tau_0) - eF\tau$ . Provided that the electrons and holes do not tunnel into adjacent bands the Houston function is a good approximation for the field-dependent states. In order to study the effect of coupling between the quantum wells we use the procedure of Voisin *et al.*,<sup>13</sup> in which the envelope functions are constructed from a linear combination of well states. This is a quasi-tight-binding scheme for the lowest energy levels and is valid if the barriers are not too thin. In this case the particles in the lowermost eigenstates will be partially confined to the well regions. Accordingly the envelope function is written as

$$f_{cn}(q, x) = \frac{1}{\sqrt{N}} \sum_p e^{ipqd} \Phi_n(x - pd), \quad (2)$$

where  $N$  is the number of wells (assumed very large) and  $\Phi_n$  is the wave function of the  $n$ th well state. Taking into account only nearest-well interactions, the dispersions relations are given by<sup>13</sup>

$$E_n = E_{n0} + 2t_n \cos(qd) + \frac{\hbar^2 \mathbf{k}_\perp^2}{2m^*}, \quad (3)$$

where  $E_{n0}$  is the energy of  $n$ th state of the isolated well,  $2t_n$  is the bandwidth of the  $n$ th subband and is a measure of the overlap between wave functions in adjacent wells. Equation (3) applies to both electron and hole states provided the appropriate values of  $E_{n0}$  and  $t_n$  are substituted. The probability of absorbing a photon is found from<sup>14</sup>

$$w = \left[ \frac{e}{mc} \right]^2 \left| \int_0^\tau d\tau' \int dr \Psi_{cn}^*(k', r) \mathbf{A} \cdot \mathbf{P} \Psi_{vm}(k, r) \right|^2, \quad (4)$$

where  $\Psi_{vm}$  is the wave function for the  $m$ th valence band state. After finding the probability per unit time for a valence- to conduction-band transition, the total transition rate per unit volume is obtained by summing over all initial states as follows:

$$W = \frac{1}{(2\pi)^3} \int d\mathbf{k}_\perp dq \left[ \frac{dw}{d\tau} \right]. \quad (5)$$

Substituting (1) in (4),

$$w = \left[ \frac{e}{mc} \right] A_0^2 \left| \int_0^\tau d\tau' M_{cv} I_{mn}(q) \exp \left[ -\frac{i}{eF} \int_0^q [E_n(\mathbf{k}_\perp, q') - E_m(\mathbf{k}_\perp, q') - \hbar\omega] dq' \right] \right|^2, \quad (6)$$

where  $E_n$  and  $E_m$  are, respectively, the dispersion relations for the conduction and valence states. Explicitly the momentum matrix element  $M_{cv}$  is given by

$$M_{cv} = \int d\mathbf{r} u_c^*(\mathbf{r}) \hat{\mathbf{e}} \cdot \nabla u_v(\mathbf{r}), \quad (7)$$

and the overlap integral  $I_{mn}$  between the  $m$ th valence- and the  $n$ th conduction-band states is found from

$$I_{mn}(q) = \int dx f_{cn}^*(q, x) f_{vm}(q, x). \quad (8)$$

As shown in Ref. 13,  $I_{mn}$  is weakly dependent on  $q$  for transitions between states of the same parity and is negli-

gible for transitions between states of different parity. In the following scheme we consider transitions for the case of  $m=n$  and for odd values of  $n$ .

#### A. Photon energy less than the effective band gap

Here the effective band gap  $E_0$  is defined as  $E_0 \equiv [E_{n0}(\text{electron}) + E_{n0}(\text{heavy hole}) + E_g]$  where  $E_{n0}$  has been defined in Eq. (3) and  $E_g$  is the band gap of GaAs. From Eq. (6) the band-to-band transition probability is given by

$$w = \left[ \frac{e}{m^*c} \right]^2 A_0^2 \left| \int_{-\pi/d}^{\pi/d} \frac{dq}{eF} M_{cv} I_{nn} \exp \left[ \frac{-i}{eF} \int_0^q dq' (E_{ne} - E_{nh} - \hbar\omega) \right] \right|^2. \quad (9)$$

Subscripts  $e$  and  $h$  have been added to the energies to denote electron and hole states. The integrand in (9) has saddle points  $q_s$  for small fields when  $E_n(\mathbf{k}_\perp, q) - E_m(\mathbf{k}_\perp, q) - \hbar\omega = 0$ . These occur in the complex  $q$  plane and are obtained from:

$$\cos(q_s d) = \frac{2m_{cv}^*(E_0 - \hbar\omega) + \hbar^2 \mathbf{k}_\perp^2}{4m_{cv}^* t} \equiv r, \quad (10)$$

where  $m_{cv}^*$  is the joint density-of-states effective mass, and  $2t$  is the sum of the two mini-bandwidths. Depending on whether  $r$  is greater or less than 1, the position of the saddle points in the  $q$  plane will vary. Figure 1(a) shows the saddle points in the complex  $q$  plane for the case  $r > 1$ . The integration in Eq. (9) is over the first mini-Brillouin zone which extends from  $q = -\pi/d$  to  $q = \pi/d$ ,  $d$  being the superlattice period. Provided there are no poles or branch points in between, the path of integration in Eq. (9) can be deformed to include the appropriate saddle point as shown in Fig. 1(a). Of the two saddle points  $\pm q_s$  in the first miniature zone,  $-q_s$  is more important because it occurs at a higher level than  $+q_s$ . The integrand is negligibly small at  $+q_s$  but has a nonzero value at  $-q_s$ . There are then two contributions to the integral. The principal contribution comes from the saddle point and yields terms of the order of  $\sqrt{F}$ , while the other contribution comes from the endpoints and produces terms of the order of  $F$ . Based on the initial assumption of small  $F$ , the endpoint contribution can be neglected. Substituting the results in Eq. (5) we obtain the total transition rate. It is noted that  $w$  is independent of  $q$ . Therefore the integration with respect to  $q$  in (5) is simply the length of the mini-Brillouin zone. Also, the probability per unit time required in (5) is found by dividing  $w$  by the time taken by the electron to traverse the miniature zone. After making the appropriate substitutions we obtain

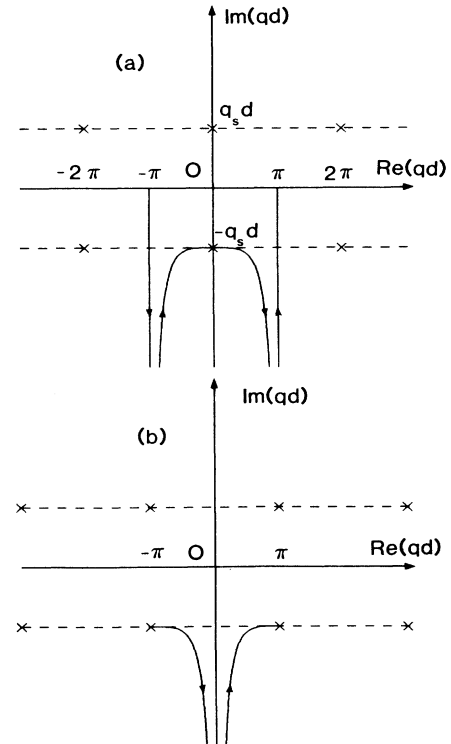


FIG. 1. (a) Sketch of the complex  $q$  plane. Because of periodicity, an infinite number of saddle points are present. The dashed lines represent the imaginary parts of the saddle points, which are constant.  $q_s$  and  $-q_s$  are the two saddle points in the first mini-Brillouin zone which extends from  $q = -\pi/d$  to  $\pi/d$ . The path of integration from left to right is deformed to pass through the path of steepest descent. The three contours shown correspond to the contributions to the total integral. (b) Showing the saddle points  $q_s$  in the complex  $q$  plane at which the adjacent subbands are joined. As in Fig. 1(a), all the points lie on the dashed lines. For the case  $E_0 > 2t$  the points are located at the zone boundary. The solid lines indicate the path of integration.

$$W = \frac{KM_{cv}^2 I_{nn}^2}{d} \int_{r_0}^{\infty} \frac{dr}{(r^2-1)^{1/2}} \exp \left[ -\frac{4tr}{eFd} \left[ \cosh^{-1} r - \frac{(r^2-1)^{1/2}}{r} \right] \right], \quad (11)$$

in which  $r_0 = (E_0 - \hbar\omega)/2t$  and  $K = (e/mc)^2 (2\pi)^2 A_0^2 m_{cv}^* / \hbar^3$ . If  $r_0 < 1$ , the path of integration along  $r$  circles the branch point at  $r=1$ . Allowance must be made for the case of  $r_0 < 1$  (i.e., the presence of saddle points on the real  $q$  axis). The final results are obtained by numerical integration of the following equation:

$$W = \frac{KM_{cv}^2 I_{nn}^2}{d} \left\{ H(r_0-1) \int_{\cosh^{-1} r_0}^{\infty} dx \exp \left[ -\frac{4t}{eFd} (x - \tanh x) \cosh x \right] \right. \\ \left. + H(1-r_0) \left[ \int_0^{\cosh^{-1} r_0} dx \cos^2 \left[ \frac{2t}{eFd} (x - \tanh x) \cosh x - \frac{\pi}{4} \right] \right. \right. \\ \left. \left. + \int_0^{\infty} dx \exp \left[ -\frac{4t}{eFd} (x - \tanh x) \cosh x \right] \right] \right\}, \quad (12)$$

where

$$H(z) = 1; \quad z > 0, \\ = 0; \quad z < 0.$$

If  $E_0 \gg \hbar\omega$  and the field is very small, Eq. (12) can be solved by successive integration by parts. Then the leading term is given by

$$W = KM_{cv}^2 I_{nn}^2 eF \frac{\exp \left[ -\frac{4tr_0}{eFd} (\cosh^{-1} r_0 - 1) \right]}{(E_0 - \hbar\omega) \cosh^{-1} r_0}. \quad (13)$$

The higher-order terms contain increasing powers of  $F$  and  $1/E_0$  in the prefactor and are therefore negligible. Equation (13) exhibits the same field dependence as the Franz-Keldysh result for bulk material.<sup>6,7</sup> However the dependence on  $\hbar\omega$  is more complicated for the superlattice case. There are now terms involving the superlattice

bandwidth  $t$ . In general this parameter is of the order of a few meV, a consequence of electron localization in the well regions. Owing to the quasi-two-dimensional electron transport, Eqs. (12) and (13) yield different results for the absorption coefficient than for bulk GaAs. An additional term is the overlap integral  $I_{nn}$ .

#### B. Photon energy greater than the effective band gap

As in the preceding section the transition probability is calculated by the saddle-point method. In counting the total number of transitions  $W$ , we need to account for the fact that the saddle point can occur at various points of the  $q$  plane (depending on the value of  $r$ ), being real in some instances and complex in others. It implies that the deformed path of integration is not the same in every instance and must be worked out for each case. Thus the final solution is piecewise and can be worked out as before,

$$W = \frac{KM_{cv}^2 I_{nn}^2}{d} \left\{ H(x_0-1) \left[ \int_0^{\cosh^{-1} x_0} dx \cos^2 \left[ \frac{2\pi t}{eFd} \cosh x \right] \exp \left[ -\frac{4t}{eFd} (x - \tanh x) \cosh x \right] \right. \right. \\ \left. \left. + \int_0^{\pi/2} dx \cos^2 \left[ \frac{2t}{eFd} (\pi - x + \tanh x) \cos x - \frac{\pi}{4} \right] \right] \right. \\ \left. + H(1-x_0) \int_{\cosh^{-1} x_0}^{\pi/2} dx \cos^2 \left[ \frac{2t}{eFd} (\pi - x + \tanh x) \cos x - \frac{\pi}{4} \right] \right. \\ \left. + \int_0^{\pi/2} dx \cos^2 \left[ \frac{2t}{eFd} (-x + \tanh x) \cos x - \frac{\pi}{4} \right] + \int_0^{\infty} dx \exp \left[ -\frac{4t}{eFd} (x - \tanh x) \cosh x \right] \right\}. \quad (14)$$

Here  $x_0 \equiv (\hbar\omega - E_0)/2t$  and the function  $H(z)$  has the same meaning as before. The foregoing results pertain to transitions for odd values of  $n$ . When  $n$  is even Eqs. (12)–(14) are only slightly modified.

### III. INTERBAND TUNNELING

A recent article<sup>15</sup> has justified the use of Houston functions for bulk material on the grounds that the interband

coupling is small for typical values of electric field. In this section we calculate the tunneling probability between adjacent subbands in either the conduction or valence bands. Using the crystal momentum representation (CMR) (Ref. 16) of Schrödinger's equation, we find that the interband matrix element linking states of equal energy is obtained from

$$M_{nm} = \frac{eFd}{2\pi} \int dq X_{nm} \exp \left[ \frac{i}{eF} \int_0^q (E_n - E_m) dq' \right], \quad (15)$$

$$X_{nm} = i \int f_n^*(k_{\perp}, q) \frac{\partial f_m(k_{\perp}, q)}{\partial q} dr, \quad (16)$$

where the  $f_n$  are the normalized and orthogonalized envelope functions representing the conduction- or valence-band-edge perturbations, and the  $E_n$  are the dispersion relations defined previously. We consider the specific case

$$T \approx \frac{2\pi eF}{d(\epsilon_0^2 - 4t^2)^{1/2}} \cos^2 \left[ \frac{\pi \epsilon_0}{eFd} \right] \exp \left[ -\frac{\epsilon_0}{eFd} \left( \cosh^{-1} \frac{\epsilon_0}{2t} - \frac{(\epsilon_0^2 - 4t^2)^{1/2}}{\epsilon_0} \right) \right]. \quad (19)$$

Equation (19) is valid as long as  $\epsilon_0 > 2t$ . For  $\epsilon_0 < 2t$ ,  $T$  is given by

$$T \approx \frac{2\pi eF}{d\sqrt{4t^2 - \epsilon_0^2}} \cos^2 \left[ \frac{\epsilon_0}{eFd} \left( \pi - \cos^{-1} \frac{\epsilon_0}{2t} \right) + \frac{\sqrt{4t^2 - \epsilon_0^2}}{\epsilon_0} - \frac{\pi}{4} \right]. \quad (20)$$

The apparent singularity at  $\epsilon_0 = 2t$  is resolved by observing that the integrand in Eq. (15) consists of a real and an imaginary part. Being an odd function, the latter yields zero over the limits of integration. However, the real part may actually be expressed in terms of Bessel functions of the first kind and produces a finite contribution for all  $\epsilon_0$ . When  $\epsilon_0 < t$  the two subbands overlap in which case  $T$  loses its meaning as a tunneling probability. The absence of a  $k_{\perp}$  dependence in  $T$  is accounted for by noting that the interband separation is the same for all  $k_{\perp}$ : we assumed that the effective mass in the superlattice plane is independent of the subband index.  $T$  vanishes when  $\epsilon_0 = eFd/2$ . This is plausible if the electron oscillates between adjacent subbands.

For typical subband separations of about 200 meV and bandwidths of about 8 meV,  $T$  is less than  $10^{-2}$  for fields below 180 kV/cm.  $T$  will, of course, approach 1 for higher-order subbands which tend to be closely spaced.

#### IV. RESULTS AND DISCUSSION

Apart from a constant factor, Eqs. (12) and (14) represent the absorption coefficient. We have computed  $W$  for various superlattice geometries and have sketched the results in Figs. 2–5. Only  $n=1$  transitions are shown. Figure 2 treats the case of a superlattice of period 100 Å and well widths of 50 Å. Because of the two-

of tunneling between the  $n=1$  and  $n=2$  conduction subbands. From the preceding section,

$$E_2 - E_1 = \epsilon_0 + 2t \cos(qd), \quad (17)$$

in which  $\epsilon_0$  is defined as the energy separation between the first two discrete levels of the isolated quantum well and  $2t$  is the sum of the widths of the associated subbands. The two subbands are joined in the complex plane at saddle points  $q_s$  defined by  $\cos(q_s d) = -\epsilon_0/2t$ . For small  $F$ , Eq. (15) can be solved asymptotically since the saddle-point contributions will be dominant [see Fig. 1(b) for a sketch of the  $q$  plane and the paths of integration].  $M_{12}$  is obtained by adding the two contributions shown in Fig. 1(b). The tunneling probability  $T$  is found from<sup>17</sup>

$$T = \frac{2\pi}{\hbar} |M_{12}|^2 \rho(E) \frac{2\pi\hbar}{eFd}. \quad (18)$$

Here  $\rho(E)$  is the density of states and is given by  $1/eFd$ . After making the appropriate substitutions in (18) we obtain

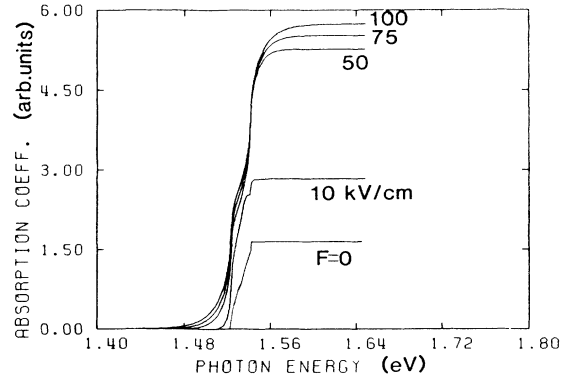


FIG. 2. Absorption coefficient versus photon energy for  $n=1$  heavy-hole electron transitions for a well width of 50 Å and a barrier width of 50 Å. The zero-field case is compared with four cases of applied field. (See also Ref. 13 for a sketch of the zero-field case.) The superlattice is GaAs-Ga<sub>0.7</sub>Al<sub>0.3</sub>As which is assumed to have a conduction-band-edge discontinuity of 0.25 eV and a valence-band-edge discontinuity of 0.15 eV.

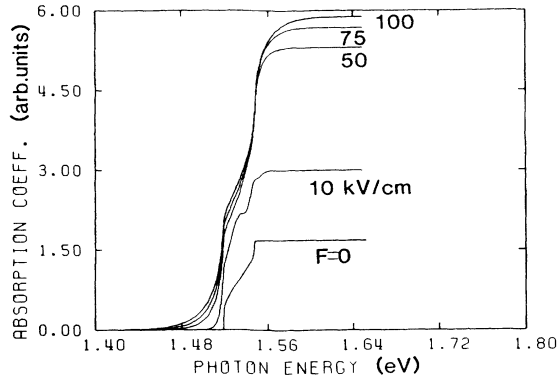


FIG. 3. Absorption coefficient as a function of photon energy for  $n=1$  transitions for a well width of 50 Å and a barrier width of 40 Å. The values of electric field are the same as in Fig. 2.

dimensional electron confinement caused by such relatively thick barriers, the absorption coefficient resembles a step function, as in the case of an MQW. For comparison, the zero-field case is included. In the limit as the field tends to zero, the results approach the zero-field case, and are marked by a Van Hove singularity at a value of  $\hbar\omega$  equal to the effective band gap plus the sum of the electron and hole subband widths. As expected, the absorption edge in the zero-field case is abrupt. Both the singularity and the absorption edge are smeared out once the field is applied, with the edge becoming an exponential tail. If the electrons and holes were not free to tunnel out of the wells, the abruptness of the edge would persist even for very high fields. In Fig. 3 the barrier layers have been reduced to 40 Å, and in Fig. 4 they have been further reduced to 20 Å. As the barriers become thinner the red shift is enhanced, as shown in Fig. 5. This is caused by the broadening of the subbands which leads to a reduction of the effective superlattice band gap. Energy-level

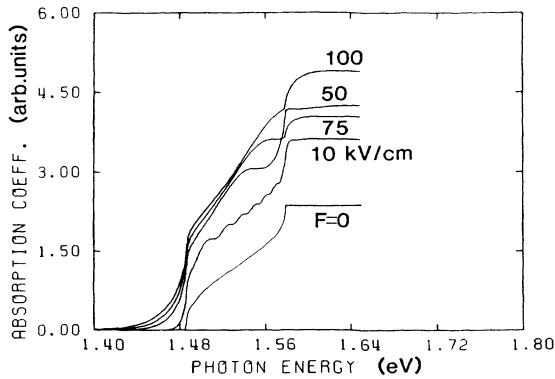


FIG. 4. Absorption coefficient as a function of photon energy. The barrier width has been reduced to 20 Å. Close coupling between the wells gives rise to Franz-Keldysh oscillations. As  $F$  increases the amplitude and period become larger.

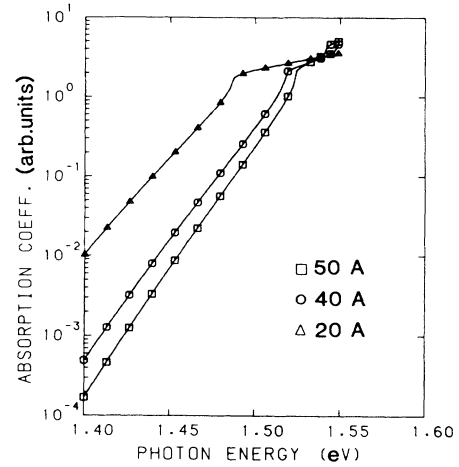


FIG. 5. Absorption coefficient as a function of photon energy for three cases of barrier widths. The well width is 50 Å and the electric field in each case is 100 kV/cm. An increase in the red shift is shown for thinner barriers.

broadening also causes the onset of constant absorption to occur at a higher value of  $\hbar\omega$ , as shown more clearly in Fig. 4, for 20-Å barriers. As the barrier thickness is reduced the dispersion relations of Eq. (3) will be less reliable since the electrons and holes become delocalized. However, we feel that the formalism is still valid provided the correct band structure is inserted in the limit of extremely thin barriers. In each of the three cases shown the absorption coefficient is expected to increase with increasing field because vertical transitions in  $q$  space can occur between any given pair of states, unlike the zero-field case.

The Franz-Keldysh shift for  $\hbar\omega < E_0$  is clearly shown. In this case the absorption tail is caused by the penetration of the wave functions into the forbidden gap as in the bulk case. An additional correction to the energies not easily recoverable from the Houston formalism may be found from the CMR and can be calculated from<sup>17</sup>

$$E_n^{(1)}(\mathbf{k}_\perp, q) = E_n(\mathbf{k}_\perp, q) - eFX_{nn}(\mathbf{k}_\perp, q). \quad (21)$$

The superscript in Eq. (21) denotes first-order correction.  $E_0$  is expected to be reduced by a few meV and will cause a noticeable shift for  $\hbar\omega < E_0$ .

As the wells become more closely coupled, a ladderlike behavior occurs as seen in Fig. 4. We believe that these are Franz-Keldysh oscillations which may be compared with the oscillatory absorption coefficient for bulk GaAs. (See, for example, the bulk calculations of Ref. 8.) For bulk GaAs the oscillations appear as points of inflection in the absorption versus photon energy curves, and are possibly caused by the oscillatory nature of the overlap between valence and conduction states as a function of  $\hbar\omega$  and  $F$ . In the superlattice case, we find that both the am-

plitude and period of the oscillations become larger as the field is increased. This is also true for the bulk case. In Fig. 4, the apparent disappearance of the oscillations as the field is increased from 10 to 100 kV/cm, is explained by noting that their amplitudes and periods are actually greater when the field is increased, and that they occur only between the effective band gap and the Van Hove singularity. The oscillatory behavior is a direct consequence of coupling between the wells and it vanishes as the barrier height or thickness of the Ga<sub>1-x</sub>Al<sub>x</sub>As layer is increased, as shown in Figs. 2 and 3. Therefore, in the limit of thin barriers we believe that our results show aspects of bulk behavior. We have shown only transitions between the  $n=1$  valence and conduction subbands. Similar results are obtained for transitions between the higher-order subbands and are simply added to Eqs. (12)–(14). For higher-order subbands, the curves are shifted to the right along the  $\hbar\omega$  axis. We have not included these results in Figs. 2–5 because the dispersion relations are increasingly in error as  $n$  becomes larger. Transitions between states of different parity can also be calculated but these are anticipated to be much smaller.

It is noted that the concept of the change in the overlap integral with increasing field is not a useful one here, since the changes induced by  $F$  are manifested as distor-

tions of the energy space. Furthermore we observe that even though the electron-hole interaction in, say, the  $j$ th well is reduced for increasing  $F$ , it is offset by the increasing interaction between holes in the  $j$ th well and electrons in the  $(j-1)$ th well.

## V. SUMMARY

In summary, we have investigated optical absorption in a GaAs-Ga<sub>1-x</sub>Al<sub>x</sub>As superlattice in the presence of an electric field. We have extended the Franz-Keldysh approach to the case of a superlattice and have calculated the transition rates between conduction and valence Houston states. The Franz-Keldysh effect and Franz-Keldysh oscillations are recovered from the model. Our investigations of tunneling between the lowest-lying subbands indicate that they are weakly coupled by the field, thereby justifying the use of the Houston functions.

## ACKNOWLEDGMENTS

B. J. acknowledges helpful discussions with Professor Dee-Son Pan. The authors have benefited from helpful discussions with Dr. Joel Schulman and Dr. Ken Brown. This work was supported in part by the Office of Naval research.

- 
- <sup>1</sup>R. T. Collins, K. von Klitzing, and K. Ploog, Phys. Rev. B **33**, 4378 (1986).
  - <sup>2</sup>H. Iwamura, T. Saku, and H. Okamoto, Jpn. J. Appl. Phys. **24**, 105 (1985).
  - <sup>3</sup>D. A. B. Miller, D. S. Chemla, T. C. Damen, A. C. Gossard, W. Wiegmann, T. H. Wood, and C. A. Burrus, Phys. Rev. B **32**, 1043 (1984); D. A. B. Miller, D. S. Chemla, T. C. Damen, A. C. Gossard, W. Wiegmann, T. H. Wood, and C. A. Burrus, Phys. Rev. Lett. **53**, 2173 (1984).
  - <sup>4</sup>C. Alibert, S. Gaillard, J. A. Brum, G. Bastard, P. Frijlink, and M. Erman, Solid State Commun. **53**, 457 (1985).
  - <sup>5</sup>D. A. B. Miller, D. S. Chemla, T. C. Damen, T. H. Wood, C. A. Burrus, A. C. Gossard, and W. Wiegmann, IEEE J. Quantum Electron. **21**, 1462 (1985).
  - <sup>6</sup>W. Franz, Z. Naturforsch. **13A**, 484 (1958).
  - <sup>7</sup>L. V. Keldysh, Zh. Eksp. Teor. Fiz. **34**, 1138 (1958) [Soviet Phys.—JETP **7**, 788 (1958)].
  - <sup>8</sup>D. A. B. Miller, D. S. Chemla, and S. Schmitt-Rink, Phys. Rev. B **33**, 6976 (1986).
  - <sup>9</sup>P. W. A. McIlroy, J. Appl. Phys. **59**, 3532 (1986).
  - <sup>10</sup>R. Dingle, A. C. Gossard, and W. Wiegmann, Phys. Rev. Lett. **34**, 1327 (1975).
  - <sup>11</sup>W. V. Houston, Phys. Rev. **57**, 184 (1940).
  - <sup>12</sup>J. Callaway, Phys. Rev. **130**, 549 (1963).
  - <sup>13</sup>P. Voisin, G. Bastard, and M. Voos, Phys. Rev. B **29**, 935 (1984).
  - <sup>14</sup>F. Bassani, *Band Structure and Interband Transitions*, Proceedings of the International School of Physics "Enrico Fermi" Course XXXIV, 1965, edited by J. Tauc (Academic, New York, 1966).
  - <sup>15</sup>J. B. Krieger and G. J. Iafrate, Phys. Rev. B **33**, 5494 (1986).
  - <sup>16</sup>E. N. Adams, Phys. Rev. **107**, 698 (1957).
  - <sup>17</sup>E. O. Kane, J. Phys. Chem. Solids **12**, 181 (1959).